Measuring fixation disparity with infrared eye-trackers

Maria De Luca
Fondazione Santa Lucia-Scientific Institute for Research
Hospitalization and Health Care
Neuropsychology Unit
via Ardeatina 306
00179 Rome, Italy

Donatella Spinelli
Fondazione Santa Lucia-Scientific Institute for Research
Hospitalization and Health Care
Neuropsychology Unit
via Ardeatina 306
00179 Rome, Italy
    and
Università degli Studi di Roma "Foro Italico"
P.le Lauro De Bosis 1
00194 Rome, Italy

Pierluigi Zoccolotti
Fondazione Santa Lucia-Scientific Institute for Research
Hospitalization and Health Care
Neuropsychology Unit
via Ardeatina 306
00179 Rome, Italy
    and
Sapienza University of Rome
Department of Psychology
via dei Marsi 78
00179 Rome, Italy

Fabrizio Zeri
Sapienza University of Rome
Department of Psychology
via dei Marsi 78
00176 Rome, Italy
    and
Roma Tre University
Faculty of Mathematics, Physics and Natural Sciences
Optics and Optometry-Department of Physics
via della Vasca Navale 84
00146 Rome, Italy

Abstract. Fixation disparity, that is, misalignment of the gaze direction of both eyes, may be observed in static conditions (through standard optometric evaluation) and dynamic conditions (through eye movement recording). A computation method is presented to determine vergence angles and fixation disparity from gaze positions as commonly recorded by infrared eye-trackers when a participant looks at a personal computer (PC) screen. Eye-tracking devices provide gaze position in coordinates relative to the bidimensional screen surface. From these data, vergence angles can be calculated by trigonometric triangulations; fixation disparity is then calculated from the vergence angles. The application of the procedure to the recordings of one participant is described. To control for the effective alignment of the two eyes on the target during binocular calibration, a procedure based on the dichoptic presentation of nonius lines was used. The recordings confirm that computation and the dichoptic calibration procedures ensure reliable measures of vergence and fixation disparity. The usefulness of this approach with infrared recording of eye position is discussed. © *2009 Society of Photo-Optical Instrumentation Engineers.* [DOI: 10.1117/1.3077198]

1 Introduction

Binocular fixation is not always perfect. When focusing on a point in space, the lines of gaze of the two eyes may not be perfectly aligned on the target and a fixation error may occur. This fixation error (called fixation disparity, or FD) is referred to as eso-disparity (or crossed disparity) when the lines of gaze cross in front of the fixation point, and exo-disparity when the lines of gaze cross behind it (uncrossed disparity).

In clinical settings, FD can be measured by subjective tests such as the Mallett test, Sheedy's disparometer, and the Borish test (for a review, see Saladin[1]). These tests are based on subjects' reports/responses during static fixation tasks. An objective measure of FD is obtained through eye movement recordings by measuring vergence angles. This measurement is taken in a dynamic condition, because data can be collected while subjects move their eyes on a personal computer (PC) screen; recording can extend over relatively long periods of time to assess stability of fixation over time.

By using scleral search coils, it is possible to obtain an accurate recording of absolute eye rotation angles, and consequently, vergence. In fact, this device has been used extensively in research on vergence (e.g., Collewijn, Erkelens, and Steinman[2]). An alternative method is infrared eye-tracking. One advantage of eye tracking is that it is not invasive and therefore is potentially useful with patients, particularly children. Infrared eye-trackers are generally provided with analysis software that determines the gaze position—that is, the projection of the line of gaze on the observed surface (generally the PC screen), not the eye rotation angle. Therefore, the

Address all correspondence to: Maria De Luca, Fondazione Santa Lucia-IRCCS, Via Ardeatina 306, 00179 Roma, Italy. Tel: +39 0651501360; Fax: +39 0651501366; E-mail: m.deluca@hsantalucia.it
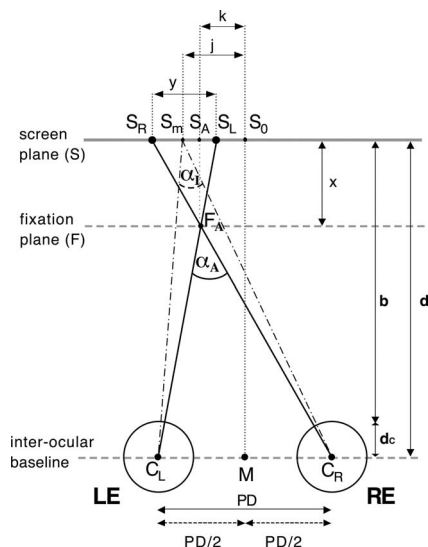
Fig. 1 Elements (planes, points, segments, and angles) involved in the trigonometric computations. The ideal vergence angle (α_I) is sketched by the black dash-dotted line; the actual vergence angle (α_A) is presented in the case of hyperconvergence (eso-disparity) by a solid black line.

Fig. 2 Ideal vergence angle; three cases are depicted. In the first case (α_{I0}), point F_{A0} (as defined in Fig. 1) is on the midline between the eyes; its projection on plane S coincides with S_0, so $j=0$ (note that S_{I0} in this figure corresponds with S_0 in Fig. 1). In the second case (α_{I1}), segment j is less than $PD/2$. In the third case (α_{I2}), segment j is greater than $PD/2$.

vergence angle is not automatically available. Note that the binocular gaze positions of the two eyes cannot be used directly to determine FD. Additional computations are needed to derive vergence angles from basic data obtained with infrared eye-trackers. Nevertheless, the commercially available analysis packages for infrared eye-trackers typically lack this feature. Furthermore, the method for deriving vergence angles from gaze position is only briefly outlined in the literature (e.g., Fajardo, Luke, and Grant[3]), and there is no explicit reference to FD.

The first goal of this study was to develop computations that would allow FD measurements from gaze positions as measured by infrared eye-trackers. In particular, equations based on trigonometric computations are described, including those for computing vergence angles. The final equation can be applied to the output data of an eye-tracking system that allows FD calculations. The computations will be presented in Sec. 2. To demonstrate how to apply this equation, we recorded binocular eye movements during a fixation task and used gaze positions as the known terms of the equation (see Sec. 3).

Another goal of this study pertains to binocular calibration. Calibration is the procedure performed before acquisition of eye movement data relative to a specific task (e.g., reading, scanning a figure, fixating a target, etc.). Calibration generally consists of recording the gaze position at known locations (i.e., fixation points that define the calibration matrix) on the PC screen. These data are used as a baseline to derive the gaze position during the experimental task.

A critical aspect of binocular recordings in general and of measuring FD in particular is to obtain reliable binocular calibrations. In fact, a prerequisite for obtaining a nonspurious measurement is that binocular calibration must be performed with the optimal alignment of lines of gaze. One method for calibrating before binocular tasks consists of making the two
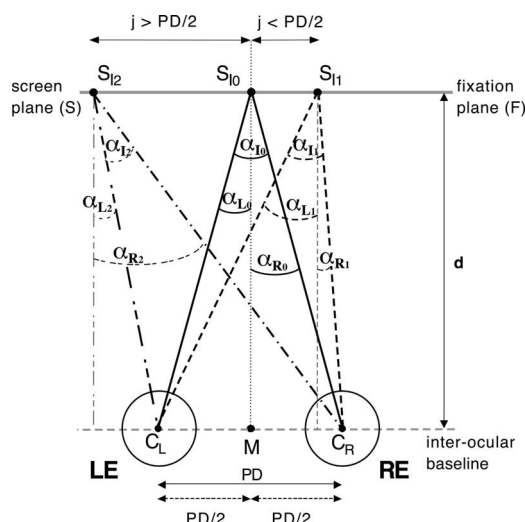
monocular calibrations "in-turn," which means the eyes are tested separately, one after the other, in monocular viewing. This method can be affected by the temporal shift between the two monocular measurements; it is also affected by a lack of control of a accurate target fixation during the calibration procedure. Therefore, in most cases good fixation during calibration is assumed but not fully controlled.

In this study, both eyes performed calibration simultaneously through an ad hoc setting developed to obtain aligned calibration data points. To check for binocular alignment during calibration, vertical nonius lines were dichoptically presented. The participant signaled when perfect alignment of the two vertical lines (seen separately by the two eyes) was reached. This procedure allowed the alignment of the lines of gaze on the calibration target, providing a baseline for measuring binocular vergence in successive tasks.

To summarize, this paper will describe: (1) trigonometric computations to determine vergence angles and FD from gaze positions, as recorded by infrared eye-trackers; and (2) an example of FD measurement based on the above computations and on the method of dichoptic binocular calibration using nonius lines.

2 Computation of Fixation Disparity

2.1 *Fixation Disparity*

FD is the difference between actual (α_A) and ideal (α_I) vergence angles [see Eq. (1)]. The former is the vergence angle measured when the observer looks at the screen (lines of gaze may align on the screen plane or beyond or before it); the latter is the theoretical expected vergence angle with perfect alignment on the screen plane (i.e., zero fixation disparity):

$$FD = \alpha_A - \alpha_I. \qquad (1)$$

The main parameters involved in the computation of α_A and α_I are sketched in Fig. 1 (where α_A is represented in a case simulating eso-disparity).

In Fig. 1, RE and LE are the right eye and left eye, respectively. The line joining the rotation centers (C_R and C_L) of the two eyes is the interocular baseline. The segment PD is the distance between the eye rotation centers C_R and C_L; since this cannot be measured directly, interpupillary distance was used. S is the PC screen plane, which is parallel to the interocular baseline; b is the distance between the screen plane and the corneal vertex; d_c is the distance between the corneal vertex and the eye rotation center;* d is the distance between plane S and the interocular baseline; it is calculated as the sum of b and d_c. M is a point midway between C_R and C_L. S_0 is the orthogonal projection of M on plane S and corresponds to the center of the horizontal meridian of the PC screen. S_R and S_L represent projections on the screen of the RE and LE lines of gaze, respectively.† S_m represents the point of ideal vergence, where S_R coincides with S_L (see dashed lines in Fig. 1). If S_R and S_L do not coincide, the lines of gaze may either cross in front of plane S (as in Fig. 1) or behind it (not represented). In either case, S_m is the midpoint of segment $S_R S_L$; y is the measure of this segment. When y is equal to zero, the binocular alignment is perfect (i.e., the lines of gaze converge on S_m); the greater y, the greater the error in convergence. j is the distance between S_0 and S_m.

In the sketched case of eso-disparity, F is the actual fixation plane; F_A is the actual fixation point; S_A is the orthogonal projection of F_A on plane S; and k is the distance between S_0 and S_A.

Of the above parameters, y, PD, and d can be collected empirically. The remaining parameters are calculated by applying trigonometric rules, as reported below.

2.2 Computation of Ideal Vergence Angle (α_I)

The ideal vergence angle (α_I) is the angle formed by the two lines of gaze when they coincide on the stimulus plane (i.e., fixation plane F coincides with screen plane S). In this case, α_I is equal to α_A, and FD is equal to zero.

Three cases of α_I will be considered.

1. Case 1: S_m coincides with S_0 (as defined in Fig. 1) and $j = 0$ (see S_{I0} in Fig. 2). The ideal vergence angle (see α_{I0} in Fig. 2) is computed as:

$$\alpha_{I0} = \alpha_{R0} + \alpha_{L0}$$

$$\alpha_{R0} = \text{ArcTan}[(PD/2)/d] \quad \alpha_{L0} = \text{ArcTan}[(PD/2)/d]$$

$$\alpha_{I0} = 2\,\text{ArcTan}[(PD/2)/d]. \quad (2)$$

---

*The value of this distance varies as a function of the eyeball size. Here, a value of 13 mm was used (according to Obstfeld).[4] This distance can be assessed with a procedure reported by Rabbetts.[5]

†The line of gaze, instead of the visual axis, is commonly used to compute vergence angle. The line of gaze is the projection of an ocular centroid (i.e., the center of an anatomic structure such as the pupil or the limbus) on the observed plane. In this study, we refer to the projection of the line of gaze on the PC screen and consider it a function of the eye rotation center. This line can be assimilated to the fixation axis, joining the fixation point to the eye rotation center (see Atchison and Smith).[6]

Note that Eq. (2) cannot be applied when S_m (as defined in Fig. 1) does not coincide with S_0. In fact, this would produce an overestimation of the vergence angle; this type of overestimation increases as a function of eccentricity (i.e., the distance from the center of the screen). Equation (2) would produce an equal vergence angle at all eccentric points along fixation plane F. By contrast, it is known that an isovergence plane is a concave surface passing through the two eye rotation centers and the fixation point.[7] Hence, for all eccentric fixation points on a flat surface, the vergence angle will (by definition) be less than that on the isovergence plane. For the above reasons, Eq. (2) is modified as follows. There are two possible cases (see α_{I1} and α_{I2} in Fig. 2):

2. Case 2: S_m does not coincide with S_0 (as defined in Fig. 1) and $j < PD/2$ (see S_{I1} in Fig. 2). In this case, α_{I1} is calculated as follows:

$$\alpha_{I1} = \alpha_{R1} + \alpha_{L1}$$

$$\alpha_{R1} = \text{ArcTan}[(PD/2 - j)/d] \quad \alpha_{L1} = \text{ArcTan}[(PD/2 + j)/d]$$

$$\alpha_{I1} = \text{ArcTan}[(PD/2 - j)/d] + \text{ArcTan}[(PD/2 + j)/d]. \quad (3)$$

3. Case 3: S_m does not coincide with S_0 (as defined in Fig. 1) and $j > PD/2$ (see S_{I2} in Fig. 2). In this case,

$$\alpha_{I2} = \alpha_{R2} - \alpha_{L2}$$

$$\alpha_{R2} = \text{ArcTan}[(j + PD/2)/d] \quad \alpha_{L2} = \text{ArcTan}[(j - PD/2)/d]$$

$$\alpha_{I2} = \text{ArcTan}[(j + PD/2)/d] - \text{ArcTan}[(j - PD/2)/d]. \quad (4)$$

Equations (3) and (4) are equivalent for computing the binocular vergence angle. They can also be applied when S_m coincides with S_0 (in this case, j is equal to zero), and also in the particular case of $j = PD/2$.

2.3 Determination of Actual Vergence Angle (α_A) from Gaze Position Recorded by Infrared Eye-Trackers

The actual vergence angle (α_A) is determined by the LE and RE lines of gaze when the observer looks at the screen.

Infrared eye-trackers provide information on the projection of the line of gaze; gaze position is represented in bidimensional coordinates relative to the surface of a PC screen.

Again, we will consider three cases:

1. Case 1: F_A, the intersection between the lines of gaze, lies on segment MS_0; its projection on plane S coincides with S_0 (see Fig. 3):

$$\alpha_A = \alpha_R + \alpha_L$$

$$\alpha_R = \alpha_L$$

$$\alpha_A = 2\alpha_R$$
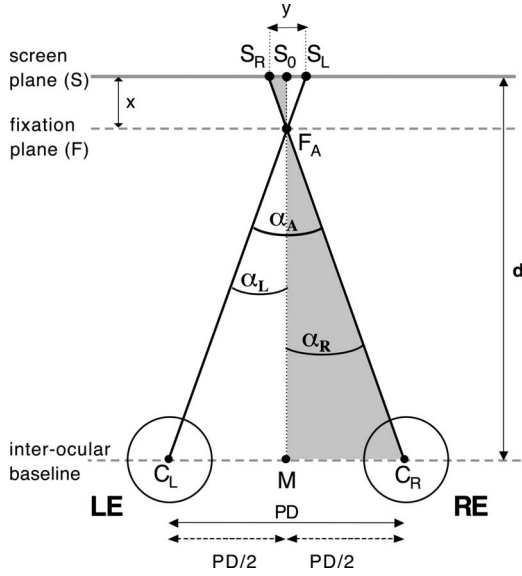
Fig. 3 Actual vergence angle α_A. In this case, point F_A lies on segment MS_0, the projection of point F_A on plane S coincides with S_0, and $k = 0$. S_0 in this figure corresponds with S_0 in Fig. 1 and S_{I0} in Fig. 2.

$$\alpha_R = \text{ArcTan}[PD/2/(d-x)]$$

$$\alpha_A = 2\text{ArcTan}[PD/2/(d-x)]. \qquad (5)$$

Considering two similar triangles $S_R S_0 F_A$ and $C_R M F_A$, we can derive

$$(PD/2)/(d-x) = (y/2)/x. \qquad (6)$$

Substituting the second term of Eq. (6) into Eq. (5) produces

$$\alpha_A = 2\text{ArcTan}(y/2x). \qquad (7)$$

The unknown value of x in Eq. (7) can be solved with the similarity of triangles method. Consider the similar triangles $S_R S_0 F_A$ and $C_R M F_A$:

$$x/(y/2) = (d-x)/(PD/2)$$

$$x = dy/(PD+y). \qquad (8)$$

Substituting Eq. (8) into Eq. (7) produces

$$\alpha_A = 2\text{ArcTan}[y/2dy/(PD+y)]$$

$$\alpha_A = 2\text{ArcTan}[y(PD+y)/2dy]$$

$$\alpha_A = 2\text{ArcTan}[(PD+y)/2d]. \qquad (9)$$

Equation (9) allows for the computation of α_A.

2. Case 2: S_{A1} is at distance $k < PD/2$ from S_0 (see Fig. 4). In this case, α_{A1} is computed as (see Fig. 4):

$$\alpha_{A1} = \alpha_{R1} + \alpha_{L1}$$

$$\alpha_{R1} = \text{ArcTan}[(PD/2+k)/(d-x)] \quad \alpha_{L1} = \text{ArcTan}[(PD/2-k)/(d-x)]$$
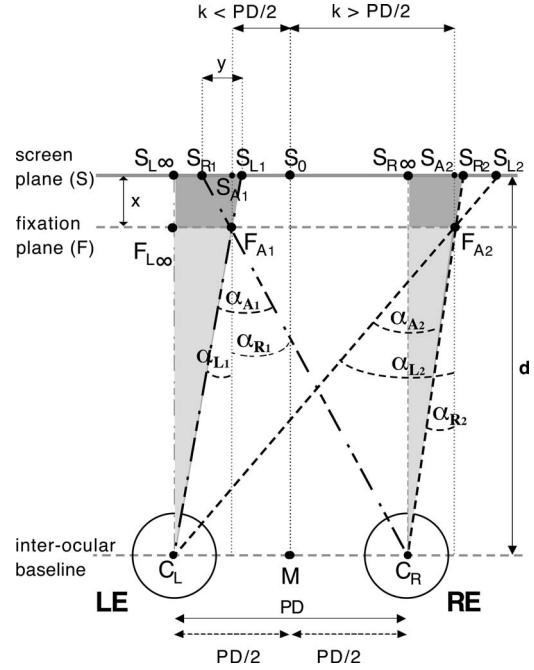
Fig. 4 Actual vergence angle; Two cases are depicted other than those for the condition presented in Fig. 3. In the first case (α_{A1}), segment k is less than $PD/2$. In the second case (α_{A2}), segment k is greater than $PD/2$.

$$\alpha_{A1} = \text{ArcTan}[(PD/2-k)/(d-x)] + \text{ArcTan}[(PD/2+k)/(d-x)],$$
$$(10)$$

where x is solved by Eq. (8), and k can be determined as

$$k = \overline{S_{L\infty}S_O} - \overline{S_{L\infty}S_{A1}},$$

where $S_{L\infty}$ is the projection on plane S of the LE line of gaze in the primary position (i.e., when looking at infinity, the lines of gaze are parallel), and S_{A1} is the projection of F_{A1} on plane S. $\overline{S_{L\infty}S_O}$ corresponds to $PD/2$:

$$k = PD/2 - \overline{S_{L\infty}S_{A1}},$$

where segment $\overline{S_{L\infty}S_{A1}}$ can be determined as

$$\overline{S_{L\infty}S_{A1}} = \overline{F_{L\infty}F_{A1}},$$

in which $F_{L\infty}$ is the projection on plane F of the LE line of gaze in the primary position. Now the equation to calculate k becomes

$$k = PD/2 - \overline{F_{L\infty}F_{A1}}. \qquad (11)$$

To determine $\overline{F_{L\infty}F_{A1}}$, consider the similar triangles $C_L F_{A1} F_{L\infty}$ and $C_L S_{L1} S_{L\infty}$:

$$(d-x)/d = \overline{F_{L\infty}F_{A1}}/\overline{S_{L\infty}S_{L1}};$$

$$\overline{F_{L\infty}F_{A1}} = \overline{S_{L\infty}S_{L1}}(d-x)/d. \qquad (12)$$

Then substitute Eq. (12) into Eq. (11):

$$k = PD/2 - \overline{S_{L\infty}S_{L1}}(d-x)/d,$$

where $\overline{S_{L\infty}S_{L1}}$ is computed as

$$PD/2 - (S_0 - S_{L1})$$

and

$$S_L - (S_0 - PD/2).$$

3. Case 3: S_{A2} is at distance $k > PD/2$ from S_0. Calculations must be reconsidered as a function of the k variation. In Fig. 4,

$$\alpha_{A2} = \alpha_{L2} - \alpha_{R2}$$

$$\alpha_{L2} = \text{ArcTan}(PD/2 + k)/(d-x) \quad \alpha_{R2} = \text{ArcTan}(k - PD/2)/(d-x)$$

$$\alpha_{A2} = \text{ArcTan}(PD/2 + k)/(d-x) - \text{ArcTan}(k - PD/2)/(d-x). \quad (13)$$

Equations (10) and (13) are equivalent and effective even for computing convergence angles when F_A lies on segment MS_0, so Eq. (10) can be used as the final equation for the actual vergence angle in all cases.

2.4 Final FD Equation

At the beginning of Sec. 2.1, FD was defined as the difference between the convergence angles α_A and α_I. Therefore, to compute FD, the final step is to substitute Eq. (1) with both Eq. (10) (computing α_A) and Eq. (3) (computing α_I):

$$\begin{aligned} FD = {} & \text{ArcTan}[(PD/2 - k)/(d-x)] + \text{ArcTan}[(PD/2 + k) \\ & /(d-x)] - \text{ArcTan}[(PD/2 - j)/d] \\ & + \text{ArcTan}[(PD/2 + j)/d]. \end{aligned} \quad (14)$$

In this final equation, the terms corresponding to an observer's interpupillary distance and viewing distance (PD and d, respectively) are known; the gaze positions (S_L and S_R) are empirically collected by eye movement recording. Then the value of y is obtained as the difference between eye gaze positions (i.e., computed as $S_L - S_R$); k is computed as $PD/2 - [S_L - (S_0 - PD/2)](d-x)/d$; x is solved with Eq. (8), i.e., $dy/(PD+y)$; and j is computed as the difference between S_0 and S_m [where the value of S_m is computed as $(S_L + S_R)/2$].

The appendix contains an example showing how to implement Eqs. (3) and (10) to calculate FD in a commonly used datasheet program (Microsoft Excel).

3 Methods

3.1 Measurement of FD during Target Fixation

This section presents an experiment in which FD was computed using Eq. (14). To obtain gaze position data (S_L and S_R), binocular eye movements were recorded in one participant as he performed a fixation task. Gaze position data S_R and S_L were used as known terms of the equation together with the participant's interpupillary distance and the viewing distance. Care was taken to perform binocular calibration. A calibration matrix with dichoptic nonius lines was used to allow eye alignment. Calibration data were acquired only when the participant perceived the alignment of nonius lines.

Then the fixation task was performed by looking at the target on the screen. To check for the goodness of the measurement, the task was repeated with a near target. To give a magnified example of lines of gaze crossing in front of the screen plane, the fixation target was displayed approximately halfway between the participant and the screen, thus producing a result that mimicked strong eso-disparity.

An actual FD approaching zero was expected when the participant looked at the far target on the screen. This expectation was due to the use of nonius lines and dichoptic alignment not only for calibration points, but also for the task fixation points. In fact, to appreciate equation efficacy, it was necessary to use a target that elicited an actual FD comparable to the ideal FD.

An eso-disparity of approximately 6 deg was expected during fixation of the near target. In fact, this target was located halfway between the screen plane and the eye plane. While S_L and S_R were referred to the PC screen, the lines of gaze crossed in front of the screen and produced a case of eso-disparity.

As shown below, mean FD while the participant looked at the screen tended toward zero, with the measured vergence angle nearly equal to the ideal vergence angle. On the contrary, while the participant looked at the near target, FD was magnified in the direction of eso-disparity, because the viewing distance reference in the equation was maintained as the eye-to-screen distance.

3.2 Participant

One of the authors, F.Z, a healthy 39-year-old male, participated in the experiment. His eyes were healthy based on direct ophthalmoscopy and slit-lamp observation. The interpupillary distance was 60 mm, and the noncyclopegic autorefractometry measure (Retinomax 2; Nikon) was OD sf +0.50cil-0.25ax5°, OS sf+0.50cil-0.50167°. His uncorrected monocular visual acuity was 20/18 (corresponding to -0.05 logMar; MAR=minimum angle of resolution), and his sighting eye (tested by the hole-in-the-card test, according to Griffin and Grisham[8]) was right. Based on von Graefe's method of measurement, the values of far and near horizontal heterophoria were 2.0^Δ exo and 10.0^Δ exo, respectively.[1] The accomodative convergence/accomodation (AC/A) ratio, measured with the gradient method, was $2^\Delta/1$. The blur, break, and recovery of convergence at far distance were 11^Δ, 29^Δ, and 9^Δ, respectively, and the break and the recovery of divergence were 10^Δ and 6^Δ. At the near distance, the values of the break and the recovery of convergence were 29^Δ and 19^Δ, and those of divergence were 22^Δ and 17^Δ. All measurements of fusional ranges were obtained using a rotary prism.[1] F.Z. was negative on the Worth four-dot test (both far and near distance) and had normal stereo-acuity (40″ of arc) measured with Wirt rings at 40 cm. On the Borish vecto-graphic near point card, he showed no fixation disparity.

3.3 Stimuli

3.3.1 Calibration stimuli

A 2×2 calibration matrix subtending 20×10 deg of visual angle at 60-cm distance was displayed on the PC screen. The calibration points were four dots subtending 0.03 deg each. Two vertically aligned nonius lines were located above and
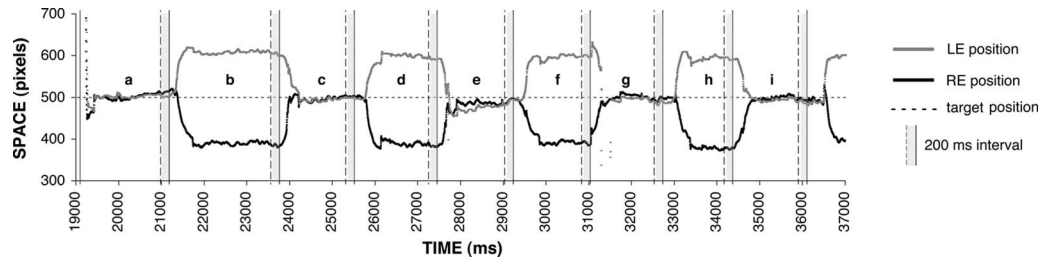
Fig. 5 RE (black line) and LE (gray line) traces during the fixation task. The solid vertical black lines represent the key press events. The dotted vertical lines are plotted 200 ms before each solid line to highlight the time interval (gray area) considered in taking average eye positions. Sectors *a, c, e, g,* and *i* represent gaze positions when looking at the far target on the screen plane; sectors *b, d, f,* and *h* represent gaze positions when looking at the near target.

below each dot. Each line subtended 3.2 deg vertically at a distance of 60 cm. The gap between upper and lower vertical lines was 0.29 deg. The four pairs of nonius lines were covered with polarizing filters; the filter covering the top line was orthogonal to the filter covering the bottom one. Two polarized filters (orthogonally oriented with respect to each eye) were fixed in front of the participant's eyes externally to the forehead-rest of the eye-tracker.

3.3.2 *Fixation stimuli*

The fixation target was a black dot. It was displayed at two viewing distances: 60 cm and 27.7 cm. At 60 cm, the target subtended 0.03 deg and was displayed on the center of the PC screen. Above and below the fixation target, two vertically aligned (gap 0.29 deg) nonius lines, subtending 3.2 deg each, were displayed on the screen. Two orthogonally oriented polarized filters covered the nonius lines. At 27.7 cm, the target subtended 0.06 deg and was printed on a transparent glass surface. Two vertically aligned nonius lines, subtending 3.6 deg each, were also printed on the same surface (gap 0.41 deg). This set of nonius lines was also covered with two orthogonally oriented polarizing filters. Far and near targets were simultaneously present.

3.4 *Apparatus*

Horizontal LE and RE movements were simultaneously recorded by an ET4 Infrared Eye Tracking System (AMTech, Weinheim, Germany). The sampling rate was 500 Hz. At best, the system has a horizontal resolution of 5 arcmin, and, as reported by the manufacturer, it is linear over a 20-deg range. The output of the recording system is represented by the projections of the LE and RE lines of gaze on the PC screen (points S_L and S_R in Fig. 1).

3.5 *Procedure*

The participant sat on a chair in front of the PC screen. A forehead rest, strap-band head rest, chin rest, and bite bar were used. He tried to avoid blinking during recording. The calibration procedure was carried out immediately before each experimental trial. The participant fixated the upper-left calibration point out of the 2×2 calibration matrix while trying to align the dichoptic nonius lines. When alignment was perceived and stabilized, he pressed a key to signal the recording system to acquire that position as a reliable binocular calibration datum. Then he had to saccade to the next calibra-

tion point (upper right) and repeat the alignment procedure. The calibration sequence (upper left, upper right, lower left, lower right) was repeated twice. Immediately after calibration, the task was performed. The participant had to saccade to the far target. His task was to maintain fixation on the far target and press a key (connected to the recording system) to track from the moment when he was able to keep the nonius lines aligned. Then he had to switch his gaze to the near target. Again, he had to press the key to signal alignment on the near fixation target, then return to fixate the far target. Each sequence of shifts lasted about 30 sec (calibration excluded). No time constraint was applied, so the number of shifts from the far to the near target varied in each sequence (on average, approximately 16 shifts per sequence). Each sequence started with a new calibration. Overall, 3 sequences were performed.

3.6 *Analysis*

The projections on the screen of the LE and RE lines of gaze (points S_L and S_R, respectively, in Fig. 1) were the output of the recording system. The S_L and S_R positions (sampled every 2 ms) were averaged across a 200-ms interval starting from 200 ms before the key press (an interval took into account the response time for key pressing after alignment). The horizontal FD was calculated by applying Eq. (14). Known terms of the equation were *PD* (6.0 cm), *d* (60.0 cm), and S_L and S_R, averaged separately (across time). Twelve fixations on the far target and (separately) 12 fixations on the near target were included in the analyses. Positive values of FD corresponded to eso-disparity (i.e., crossed lines of gaze); negative values corresponded to exo-disparity (i.e., uncrossed lines of gaze).

4 Results

An excerpt of the traces recorded during the fixation task is presented in Fig. 5. The LE trace is gray, and the RE trace is black. The figure shows a clear alternation between fixation on the far target (portions *a, c, e, g,* and *i* of the figure) and fixation on the near target (*b, d, f,* and *h*). Solid vertical lines represent the key press events; the gray areas between these lines and the closest dotted vertical lines represent the 200-ms intervals considered in the data analysis.

When the participant fixated the far target, mean FD was −0.02 deg (SD=0.18). Eight out of 12 fixations were slightly

Fig. 6 Example of datasheet with computations of α_I, α_A, and FD.

in exo-disparity (mean FD=−0.12 deg; SD=0.09; range: −0.27 to −0.01) and four were in eso-disparity (mean FD =0.19 deg; SD=0.12; range: 0.01 to 0.27).

The fixations made to converge on the near target appeared in eso-disparity (mean FD=6.19; FD=0.23; range: 5.81 to −6.56). This is because gaze position was given by S_L and S_R measured on the PC screen (see plane S in Fig. 1). These values correspond to what is expected when one looks at a 60 cm viewing distance, crossing the lines of gaze at 27.7 cm from the eye surface.

As expected, when the participant fixated the far target, his FD oscillated around zero and never exceeded ±0.3 deg. Note that reports on the limit of the horizontal meridian of Panum's area are variable, with estimates ranging from 0.1 to 0.4 deg.[9–11] Therefore, the range obtained in the present study is generally compatible with these reports. It is also consistent with the values of FD measured during the static optometric assessment carried out on the same participant.

When fixating the near target, a mean eso-disparity of 6.19 deg (with respect to the alignment that characterizes fixation on the far target) was apparent. This confirms the efficacy of the equation in a case of disparate fixation.

5 Discussion

The trigonometric computations presented here allow the measurement of FD from a gaze position. This is the type of output commonly provided by a binocular eye-tracking system based on infrared refraction. Based on Eq. (14), gaze position coordinates, interpupillary distance, and viewing distance are sufficient to calculate both the ideal and actual vergence angles, and hence FD. An example of how to compute FD using a common datasheet is provided in the Appendix.

The set of equations described in this paper contain two relevant features. First, it takes into account a parameter, such as individual interpupillary distance, which is an important

variable not always implemented in software for data analyses. Second, the eccentricity of gaze position when looking at the central zone of a PC screen, or at a more peripheral area with respect to the center of the observed plane, is taken into account in the computation to avoid overestimating convergence in the determination of vergence.

A critical concern for binocular eye movement recordings is calibration. In fact, calibration represents the baseline for computing FD in the task; indeed, the effective alignment of the eyes during calibration is mandatory in binocular recordings. In several studies, this issue was addressed using separate monocular calibrations (e.g., Liversedge et al.[12]). This method, however, can be biased due to the temporal distance between three successive measurements: first, calibration for one eye; second, calibration for the other eye; third, binocular recording during the task. On the other hand, monocular calibrations may be biased by the subjective impression of fixating accurately. Any misalignment during calibration will directly affect the amount of FD in a specific task. The use of dichoptic nonius lines during calibration guides the eyes to effectively align on the calibration target by requiring the observer to view the separate lines as aligned. In the present experiment, the dichoptic nonius lines were applied not only to the calibration stimuli, but also to the fixation stimuli. In fact, we wanted to determine whether the computation of FD was effective at predefined vergence values. For this purpose, we used the target on the PC screen as the stimulus for ca. zero FD, and the near target as a stimulus mimicking a condition of hyper-convergence (with an expected value of disparity). Under standard conditions, the nonius lines and the polarized filters are necessary only as calibration stimuli and are not used during the experimental task when the eyes are free to adopt their spontaneous FD. Thus, we propose that dichoptic calibration with nonius lines is a comparatively simple procedure that can be used with infrared eye-trackers to reliably measure FD.

Of course, one problem in obtaining accurate binocular recordings is that individuals with inefficient binocular coordination may not be able to align both eyes on the calibration targets. This limitation is present in general and also applies to the calibration procedure presented here. Nevertheless, if the observer is able to make the alignment (which can be assessed by standard optometric screening), the use of a dichoptic presentation of nonius lines during calibration may be effective for every kind of binocular recording device.

In conclusion, the application of the procedure described here for infrared eye-tracking devices allows the measurement of vergence and FD with a recording system that is less invasive than scleral search coils. This allows for testing FD in populations (such as children) in which the search coil technique cannot be easily applied, thus significantly enlarging the research perspectives on binocular eye movement recordings.

Appendix

An example of the computation of α_A, α_I, and FD (in degrees) in a common datasheet (Microsoft Excel) is reported in Fig. 6. The white columns (A, C, F, G, and H) contain values collected by the experimenter: PD=0.06 m, b=0.6 m, gaze position data for LE and RE are in meters, and S_0=0.15 m, respectively. In this example, the upper left corner of the screen is the origin of the coordinates system (expressed here in meters). The gray columns (B, D, E, I, K, L, and M) contain functions or constants. The function in column B is the value reported in column A divided by 2. Column D always contains the invariant value of 0.013 m (see Obstfeld).[4] The function in column E is the algebraic sum of columns C and D (b plus d_c). The function in column I is the algebraic sum of columns F and G (S_L minus S_R) divided by 2. The functions in columns K and L compute α_I and α_A, respectively. Finally, the function in column M is the algebraic sum of the results of column K and L (α_A minus α_I). Note that the syntax of the functions may vary according to the datasheet application used. In this example (based on a Microsoft Excel worksheet), the function must be spelled continuously within a single cell, removing space, blank, or return from the text.

References

1. J. J. Saladin, "Phorometry and stereopsis," in *Borish's Clinical Refraction*, W. J. Benjamin, Ed., pp. 724–773, W.B. Saunders, Philadelphia (1998).
2. H. Collewijn, C. J. Erkelens, and R. M. Steinman, "Binocular coordination of human horizontal saccadic eye movements," *J. Physiol. (London)* **404**, 157–182 (1988).
3. A. B. Fajardo, B. L. Luke, and J. W. Grant, "A technique for determining convergence in human subjects undergoing rotational acceleration using a binocular eye-tracking system," *Aviat., Space Environ. Med.* **69**(8), 750–754 (1998).
4. H. Obstfeld, *Optics in Vision: Foundations of Visual Optics and Associated Computations*, Butterworths, Sevenhoaks, England (1982).
5. R. B. Rabbetts, *Bennett and Rabbetts' Clinical Visual Optics*, 4th ed., Butterworths-Heinemann, Philadelphia (2007).
6. D. A. Atchison and G. Smith, *Optics of the Human Eye*, Butterworths-Heinemann, Edinburgh (2000).
7. H. Ono, "The combination of version and vergence," in *Vergence Eye Movements: Basic Clinical Aspects*, C. M. Schor and K. Ciuffreda, Eds., pp. 373–400, Butterworths, Boston (1983).
8. J. R. Griffin and J. D. Grisham, *Binocular Anomalies. Diagnosis and Vision Therapy*, Butterworths-Heinemann, Wouburn, MA (2002).
9. D. Fender and B. Julesz, "Extensions of Panum's fusional area in binocularly stabilized vision," *J. Opt. Soc. Am.* **57**, 819–830 (1967).
10. D. E. Mitchell, "Retinal disparity and diplopia," *Vision Res.* **6**, 441–451 (1966).
11. D. Qin, M. Takamatsu, and Y. Nakashima, "Measurement for the Panum's fusional area in retinal fovea using a three-dimension display device," *J. Light Visual Environ.* **28**, 126–131 (2004).
12. S. P. Liversedge, S. J. White, J. M. Findlay, and K. Rayner, "Binocular coordination of eye movements during reading," *Vision Res.* **46**, 2363–2374 (2006).